Interaction between tachyplesin I, an antimicrobial peptide derived from horseshoe crab, and lipopolysaccharide

Takahiro Kushibiki [a], Masakatsu Kamiya [a], Tomoyasu Aizawa[a,*], Yasuhiro Kumaki [a], Takashi Kikukawa [a], Mineyuki Mizuguchi [b], Makoto Demura [a], Shun-ichiro Kawabata [c], Keiichi Kawano [a]

[a] Graduate School of Life Science, Hokkaido University, Sapporo, Hokkaido 060-0810, Japan

[b] Faculty of Pharmaceutical Sciences, University of Toyama, 2630, Sugitani, Toyama 930-0194, Japan

[c] Department of Biology, Kyusyu University, Fukuoka, Fukuoka 812-8581, Japan

* Corresponding author. Tel.: +81 11 706 2985; fax +81 11 706 2985.

E-mail addresses: kushibiki@mail.sci.hokudai.ac.jp (T. Kushibiki), mkamiya@sci.hokudai.ac.jp (M. Kamiya), aizawa@mail.sci.hokudai.ac.jp (T. Aizawa), kumaki@sci.hokudai.ac.jp (Y. Kumaki), kikukawa@sci.hokudai.ac.jp (T. Kikukawa), mineyuki@pha.u-toyama.ac.jp (M. Mizuguchi), demura@sci.hokudai.ac.jp (M.Demura), skawascb@kyudai.jp (S. Kawabata), kawano@sci.hokudai.ac.jp (K. Kawano)

Abstract

Lipopolysaccharide (LPS) is a major constituent of the outer membrane of Gram-negative bacteria and is the very first site of interactions with antimicrobial peptides (AMPs). In order to gain better insight into the interaction between LPS and AMPs, we determined the structure of tachyplesin I (TP I), an antimicrobial peptide derived from horseshoe crab, in its bound state with LPS and proposed the complex structure of TP I and LPS using a docking program.

CD and NMR measurements revealed that binding to LPS slightly extends the two β-strands of TP I and stabilizes the whole structure of TP I. The fluorescence wavelength of an intrinsic tryptophan of TP I and fluorescence quenching in the presence or absence of LPS indicated that a tryptophan residue is incorporated into the hydrophobic environment of LPS. Finally, we succeeded in proposing a structural model for the complex of TP I and LPS by using a docking program. The calculated model structure suggested that the cationic residues of TP I interact with phosphate groups and saccharides of LPS, whereas hydrophobic residues interact with the acyl chains of LPS.

key words:

Antimicrobial peptide, Docking calculation, Lipopolysaccharide, NMR, Tachyplesin I

Abbreviations:

AMPs, antimicrobial peptides; CD, circular dichroism; DPC, dodecylphosphocholine; HPLC, high performance liquid chromatography; LPS, lipopolysaccharide; MALDI, matrix assisted laser desorption ionization; NMR, nuclear magnetic resonance; TOCSY, total correlation spectroscopy; TOF MS, time of flight mass spectroscopy; TP I, tachyplesin I; Tr-NOESY, transfer nuclear Overhauser effect spectroscopy; RMSD, root-mean-square deviation.

1. Introduction

Gram-negative bacteria have two kinds of membranes, an inner or cytoplasmic membrane composed of phospholipid bilayer and an outer membrane. The outer membrane of Gram-negative bacteria contains lipopolysaccharide (LPS) as a major component [1]. LPS occupies more than 90% of the outer membrane [2]. LPS consists of three distinct domains: the proximal, which is a hydrophobic lipid A region consisting of acyl chains connected to two phosphorylated glucosamine residues (GlcN); the distal, which is a highly variable polysaccharide moiety called the O-antigen; and a core oligosaccharide region that is covalently linked to the other two regions [1]. LPS is well known as an endotoxin, the inflammatory properties of which cause fatal septic shock in humans [3]. Sepsis has been a serious source of mortality in many clinical cases, but no effective medical therapy has been established. To overcome sepsis, antimicrobial peptides (AMPs) that interact with LPS have recently received increasing attention in the field of drug discovery [4,5].

AMPs are ubiquitously found in living organisms [6-9] and are an important component in innate immune response. Most AMPs exhibit a wide spectrum of antimicrobial activity against Gram-negative and Gram-positive bacteria, fungi, protozoa, and viruses [10]. In general, microbes are considered to have developed little or no resistance to AMPs unlike antibiotics, which have developed marked resistance [11]. Some AMPs that interact with LPS have been reported to neutralize endotoxin [12].

When AMPs exert their antimicrobial activity against Gram-negative bacteria or neutralize endotoxin, they should interact with the outer membrane components or LPS. Structural analyses of AMPs in complex with LPS are therefore important for understanding the mechanisms underlying the action of AMPs. However, although many structures of AMPs in water have been reported, there are just a few reports on the complex structure of AMPs-LPS or the structure of AMPs in the presence of LPS [5,13,14]. Details of the interactions between AMPs and LPS and of the relationships between mechanisms of antimicrobial activity and their structures are still unclear.

Tachyplesin I (TP I) found in small granules of hemocytes of the horseshoe crab *Tachypleus tridentatus* is one of the AMPs that can bind to LPS [15,16]. TP I is a 17-residue peptide containing six cationic residues and two disulfide bonds (C3-C16 and C7-C12), and its C-terminus is amidated [15]. In water, TP I forms an antiparallel β-sheet structure [17,18]. The conformations of TP I in the presence of DPC micelles were also determined [18]. Furthermore, TP I mutants have been studied intensively. The structure of TPY4, a TP I mutant in which all the Cys residues are replaced with Tyr, has been revealed in water and in the presence of DPC micelles [18]. CDT is a mutant of TP I in which all Cys residues are deleted, and its LPS-bound structure has been determined [19]. However, the complex structure between wild-type TP I and LPS remains unclear. In order to obtain detailed structural information about the interaction between TP I and LPS, we investigated the

structure of TP I in the presence of LPS by circular dichroism (CD) measurements, fluorescence experiments, nuclear magnetic resonance (NMR) measurements and docking calculation.

2. Materials and methods

2.1. Peptide and reagents

TP I (KWCFRVCYRGICYRRCR-NH_2) was synthesized by Fmoc solid phase chemistry (Sigma Life Science). Based on the protocols of Powers *et al*. [20], we oxidized and purified TP I. In brief, TP I was dissolved in 20 mM Tris-HCl buffer (pH 8.0) and the solution was shaken for more than 24 hours at room temperature to promote disulfide bond formation by oxidation. The correctly folded TP I (C3-C16 and C7-C12) was then separated and purified by reverse-phase HPLC. Two disulfide bonds of the purified peptide were confirmed by MALDI-TOF mass spectroscopy through an observed 4 mass unit difference between the reduced and oxidized forms of TP I. Oxidized TP I solution was lyophilized and stored at -80 ºC. LPS of *Escherichia coli* O111:B4 was purchased from Sigma-Aldrich and was used without any further purification in all experiments.

2.2. Circular dichroism spectroscopy

CD spectra were recorded on a model J-725 spectropolarimeter (Jasco) using a quartz cell with a 1 mm path length. Spectra were measured at 25 ºC over the range from 190 to 250 nm at a scanning speed of 50 nm/min. TP I and LPS were dissolved in 10 mM sodium phosphate buffer (pH 7.4) and the concentrations were 30 μM and 72 μM, respectively. The contribution from the buffer was removed by subtracting the spectrum of a sample without TP I.

2.3. NMR spectroscopy

All NMR spectra were recorded either on a BRUKER DMX 500 MHz equipped with a cryo-probe or a JEOL ECA 600 MHz spectrometer. Data were processed using NMRPipe 4.1 and NMRDraw 2.3 [21] and analyzed using Sparky 3.113 software [22]. ^{1}H NMR experiments were performed at 35 ºC with a TP I concentration of 750 μM in an aqueous solution containing 50 μM LPS and 10% D_2O, pH 3.8. The spectra of TP I in free solution were acquired at 1 mM peptide concentration. The mixing times of Two-dimensional TOCSY [23] and Tr-NOESY [24] spectra were 90 and 150 ms, respectively. The interaction of TP I with LPS was examined by measurements of 1D ^{31}P NMR at 35 ºC. 0.4 mM LPS in 10% D_2O at pH 3.8 was titrated using TP I at concentrations of 0.2, 0.4, and 0.6 mM. We

confirmed that no oligomerization of the peptide is present under our experimental conditions (data not shown).

2.4. Calculation of the three-dimensional structure of TP I

In the presence and absence of LPS, a total of 216 and 110 distance restraints were acquired from the Tr-NOESY and NOESY spectra, respectively. The TP I structures with or without LPS micelles were calculated using XPLOR-NIH [25,26]. A total of 100 structures were calculated and the quality of the structures was checked with the program PROCHECK-NMR [27] for the 20 lowest-energy structures. Structures were visualized using PyMOL [28]. NMR resonance assignments for TP I in LPS and in water have been deposited in the BioMagResBank (BMRB) entry 11538 and 11539, respectively. The structural coordinates of TP I in LPS and in water have been deposited in the Protein Data Bank (PDB) ID 2MDB and 2RTV, respectively.

2.5. Tryptophan fluorescence studies

All fluorescence experiments were carried out using a 650-40 fluorescence spectrophotometer (Hitachi) and 1 cm path length cuvette.

TP I was dissolved in 10 mM sodium phosphate buffer (pH 7.4) and its concentration was 5 μM. The intrinsic tryptophan fluorescence emission spectra were obtained by titrating a stock solution of 1 mM LPS into a TP I solution. The exciting wavelength was set to 280 nm and emission was monitored from 300 to 500 nm at 25 ºC.

Fluorescence quenching experiments were performed by stepwise addition of acrylamide from a stock solution of 5 M into sample solution at 25 ºC. The sample solution contained 5 μM TP I and 12 μM LPS in sodium phosphate buffer at pH 7.4.

The results of the fluorescence quenching experiments were analyzed by fitting to the Stern-Volmer equation, $F_0 / F = 1 + K_{SV}[Q]$. F_0 and F are the fluorescence intensities at the appropriate emission wavelength in the absence and presence of acrylamide, respectively. K_{SV} is the Stern-Volmer quenching constant and [Q] is the molar concentration of acrylamide.

2.6. Docking of TP I with LPS

The structure of TP I calculated from the distance restraints of Tr-NOE was docked onto LPS by the program AutoDock 4.2 [29]. Docking calculations were carried out based on the protocols of Bhunia *et al.* [13]. The atomic coordinate of LPS (PDB ID 1QFG) used for docking calculations was obtained from the co-crystal structure of LPS and Fhu A [30]. The TP I was used as a ligand and backbone was kept rigid, whereas almost all side chains were

defined as flexible. LPS was defined as a receptor and was kept rigid. Grid maps representing LPS were constructed using 70×80×80 points, with a grid spacing of 0.375 Å and grid center of the H2 atom of the GlcN II in lipid A. Docking calculation was carried out by using a Lamarchian genetic algorithm (LGA) with a translation step of 0.2 Å, a quaternion step of 5 deg, and a torsion step of 5 deg. The maximum number of energy evaluations increased to 15,000,000. 200 LGA docking runs were performed.

3. Results

3.1. Circular dichroism spectroscopy

We measured CD spectra of TP I in the presence or absence of LPS to estimate the secondary structures of TP I, and investigated whether TP I changes its conformation by binding to LPS. First, we measured CD spectra of TP I in the presence and absence of LPS at temperatures ranging from 25 °C to 40 °C and confirmed that there were no changes in the spectra (data not shown). The horseshoe crab is a heterothermic, saltwater animal, so we adopted the result at 25 °C. The spectrum of TP I in water displayed two positive bands at 198 and 232 nm and one negative band at 211 nm (Fig. 1). These bands are indicative of a β-sheet structure and a β-turn structure. This estimated structure of TP I in water is consistent with a previous report [16]. TP I in the presence of LPS also exhibited two positive bands at 204 and 232 nm and one negative band at 212 nm (Fig. 1). This spectrum indicated that TP I retains a β-sheet structure and a β-turn structure in its LPS-bound state. If none of the conformational changes are caused by binding to LPS, the spectrum of TP I fits with that of TP I in the presence of LPS. As is obvious from the spectra, the two spectra do not completely fit each other. This suggested that TP I changes its conformation by binding to LPS.

3.2. NMR studies of TP I in an aqueous solution

Although the solution structure of TP I was already clarified [17], to compare the structure of TP I in water with its LPS-bound state under the same condition, we measured 1D ^{1}H NMR, 2D TOCSY and NOESY of TP I in the absence of LPS and determined its solution structure (data not shown). ^{1}H resonance assignments of all the amino acids were obtained by the combined analyses of TOCSY and NOESY spectra. In aqueous solution, most of the chemical shift values of $^{1}H^{\alpha}$ were shifted down-field compared with the random-coil shift values. This property indicated that TP I adopts a β-sheet structure. The NOESY spectrum showed the long range NOEs among residues C3/C16, F4/R15, F4/C16, R5/R14, R5/R15, V6/Y13, V6/R14, C7/C12 and C7/Y13. These NOEs suggested a two-stranded antiparallel structure of TP I. These results were well consistent with the

previous reports.

3.3. Tr-NOESY of TP I in its LPS-bound state

To determine the structure of TP I in its LPS-bound state, we acquired 1D ^{1}H NMR, 2D TOCSY and Tr-NOESY spectra. The line-broadening of proton resonances was caused by the addition of 0.25 mg LPS into the solutions containing TP I (Fig. 2a). This line-broadening indicates a fast or intermediate exchange between free and LPS-bound states at the NMR time scale. We decided to measure Tr-NOESY spectra of TP I in the presence of LPS under the condition by which the line-broadening of TP I resonances was observed.

Tr-NOESY has the advantage that it can be used for the structural analysis of high-molecular-weight complexes that cannot be studied by other NMR measurements due to the broad line widths [24]. The critical micelle concentration (CMC) value of LPS has been estimated to be 1.3 ~ 1.6 μM [31], and LPS forms large micelles even at low concentrations, so the structural analysis of LPS-peptide complexes has not been easy. However, the observation of tr-NOEs from the LPS-bound peptides enabled us to determine the structure of the peptides in their LPS-bound state. By contrast to the NOESY spectrum of TP I without LPS, the number of NOE cross-peaks of TP I drastically increased in the presence of LPS (Fig. 2b). The numbers of NOEs of TP I in water and in the presence of LPS are summarized in Fig. 3. The increased peaks were mainly for sequential and inter-residue (>i+1) NOEs. Figure 3 shows that the NOEs of Cys3 and Arg17 located in the N and C termini of TP I and other residues such as Ile11 and Cys12 were particularly increased by the interaction with LPS. These results indicated the possibility of the structural stabilization of whole TP I containing N and C termini in complex with LPS. In the presence of LPS, the tr-NOESY spectrum showed the long range NOEs observed under the aqueous condition as well as the peaks of W2/R17. These peaks suggested that TP I in the presence of LPS adopts an antiparallel structure like that of TP I in aqueous solution.

3.4. Three-dimensional structure of TP I with or without LPS

We calculated the TP I structure in an aqueous solution by use of 110 distance constraints of NOEs (Fig. 4a). From the backbone dihedral angles of the calculated structure, TP I was suggested to adopt an antiparallel β-sheet composed of Phe4 - Cys7 and Cys12 - Arg15. The N and C termini did not converge well when the 20 lowest energy structures were superimposed (Fig. 4a). The poor convergence of the N and C termini suggested their structural flexibility. The RMSD value of the well-defined region (Cys3-Cys16) was 0.771 Å for the backbone atoms.

The LPS-bound structure of TP I was determined by using 216 Tr-NOE-driven distance

constraints (Fig. 4b). The structural statistics are summarized in Table 1. The backbone dihedral angles suggested that the antiparallel β-sheet structure of TP I is composed of two strands of Cys3-Cys7 and Cys12-Cys16. TP I appeared to slightly extend its two β-strands by binding to LPS. The RMSD value of the well-defined region (Cys3-Cys16) was 0.632 Å for the backbone atoms. This RMSD value is smaller than that of the TP I structure without LPS, suggesting that the structure of TP I is stabilized by binding to LPS. In addition, the NMR structure showed that the backbone of the N and C termini is more rigid in LPS than in water. Further, TP I exhibited a twisted structure in the presence of LPS. In order to evaluate the twist quantitatively, we measured the $C3C^{\alpha}$-$C16C^{\alpha}$ -$C12C^{\alpha}$ -$C7C^{\alpha}$ dihedral angle of the twenty lowest-energy TP I structures. The dihedral angle in water was 12.0 ± 30.5 degrees, while that in the presence of LPS was 53.4 ± 17.3 degrees. Conformational changes in TP I occurred via an interaction with LPS, which was consistent with the results of CD measurements; these changes included the elongation of two β-strands and structural stabilization.

3.5. Tryptophan fluorescence studies

We then investigated the interaction site between TP I and LPS by using spectroscopic techniques. To determine the local environment of W2, the intrinsic tryptophan fluorescence emission wavelength was monitored. Tryptophan fluorescence is widely used to judge the polarity of the local environment [20]. In a polar environment, tryptophan fluorescence shifts toward longer wavelength. Meanwhile, in an environment of low polarity, tryptophan fluorescence shifts toward shorter wavelength (blue shift). In the absence of LPS, the maximum wavelength of tryptophan fluorescence emission was 360 nm. The tryptophan fluorescence emission maxima of TP I showed a concentration-dependent blue shift by the additions of LPS (Fig. 5a). When the concentrations of LPS were saturated, the maximum wavelength of tryptophan fluorescence emission was 332 nm. This remarkable blue shift indicated that the tryptophan residue of TP I is incorporated into the hydrophobic environment of LPS. In order to assess the degree of solvent exposure of the tryptophan residue, florescence quenching studies were carried out for TP I in the presence or absence of LPS by using acrylamide as a quencher. Figure 5b shows Stern-Volmer plots of the tryptophan fluorescence intensity of TP I with or without LPS. The values of the Stern-Volmer constants, K_{SV} for TP I 21.7 M^{-1} in water and K_{SV} for TP I in LPS 9 M^{-1}, were estimated from the slope of the Stern-Volmer plots. As shown in Fig. 5b, TP I experienced a large quenching in its free state. This large quenching indicated an exposure of tryptophan residue to the aqueous solvent. On the other hand, the quenching of tryptophan fluorescence was limited in the presence of LPS. The limited quenching indicated a reduction in the accessibility of the tryptophan residue to acrylamide by the interaction with LPS. These intrinsic tryptophan fluorescence studies demonstrated that the Trp2 or N-terminal residues

of TP I are involved in binding to the hydrophobic region of LPS.

3.6. 1D ^{1}H NMR measurement of TP I in LPS

We obtained 1D ^{1}H NMR spectra in the presence or absence of LPS to identify the residues involved in binding to LPS. Figure 6 shows a low field of the 1D ^{1}H NMR spectra. As shown in the difference spectrum in this figure, several peaks of TP I (arrows) changed their chemical shift values upon the addition of LPS evidenced by the phase changes in the difference spectrum. These peaks were assigned to the NHs of the W2, C3, and R17 residues, which are located in the N and C termini of TP I. These chemical shift changes indicated that residues located in the N and C termini of TP I are involved in binding to LPS. The suggestion that the Trp2 residue was involved in binding to LPS was consistent with the results of tryptophan fluorescence measurements and quenching studies.

3.7. 1D ^{31}P NMR measurement of LPS in the presence of TP I

In order to investigate the site of the interaction between LPS and TP I, we measured 1D ^{31}P NMR spectra of LPS with or without TP I. In the presence of TP I, LPS showed two peaks, at 2.25 ppm and at 1.44 ppm (Fig. 7). The resonance at 2.25 ppm corresponded to the diphosphate linked to GlcN of LPS and the resonance at 1.44 ppm corresponded to the monophosphate of LPS [32,33]. By the addition of TP I solution, the ^{31}P resonance of LPS at 2.25 ppm was slightly shifted upfield. On the other hand, the peak intensity of the ^{31}P resonance of LPS at 1.44 ppm was significantly changed by binding to TP I. These changes of chemical shift and peak intensity suggested that the phosphate groups of LPS are in close proximity to TP I.

3.8. Complex structure of TP I and LPS

The five lowest-energy TP I structures in the LPS-bound state calculated by the distance constraints obtained from Tr-NOE were docked with LPS by the program AutoDock ver. 4.2. The detailed structure of LPS used in the docking calculation is shown in Fig. 8a. Each docking calculation produced 200 docked structures, and we analyzed the complex structures that showed negative free energy as a result of the docking calculation. In the majority of the complex structures for which the simulation-calculated Kd values were under 100 μM, the TP I lay down on the two GlcNs of LPS (Fig. 8b, c). In the complex, some basic residues appeared to form hydrogen bonds or salt bridges with phosphate groups or saccharides. The $N^{\zeta}H$ (amino group) of Lys1 was in close proximity to the phosphate groups of LPS, and the guanidyl group or amidated C terminus of Arg17 was also located close to the same phosphate groups. The guanidyl group of the Arg14 or Arg15 residue was

close to the saccharides, which were located on the upper part of GlcNs. Close packing was observed not only between the basic residues and the phosphate groups or saccharides but also between aromatic residues and the hydrophobic region of LPS. The indole ring of Trp2 was located near the acyl chains, a constituent of lipid A. The aromatic ring of Phe4 was also in close proximity to the acyl chains of LPS and was approximately parallel to the plane of acyl chains. This docking model showed that cationic residues located in the N and C termini of TP I interact with phosphate groups or saccharides of LPS, whereas hydrophobic residues such as Trp2 and Phe4 in the N terminus interact with the acyl chains of LPS (Fig. 8c). The key residues of TP I for interaction with LPS revealed by this docking model are consistent with the results of Trp fluorescence studies and 1D ^{1}H NMR.

4. Discussion

Over the past few decades, numerous AMPs have been identified and their activities and structures investigated [6-9,34-36]. Recently, in an attempt to overcome sepsis and other diseases caused by Gram-negative bacteria, the application of AMPs to new agents has been attracting much attention. Many reports have analyzed the structures of AMPs in the presence of LPS or mimetic membrane of Gram-negative bacteria to understand the mechanism of LPS or lipid-membrane recognition in AMPs [37-39]. However, the details of the interaction between AMPs and LPS and the relationship between the mechanisms of LPS recognition and structures of AMPs have not yet been revealed.

As one of the AMPs that can bind to LPS, TP I has been intensively studied. It is well known that TP I has broad spectrum antimicrobial activity against Gram-negative and Gram-positive bacteria as well as fungi [15,40]. In water, TP I forms an antiparallel β-hairpin and amphipathic structure. Furthermore, Laederach *et al*. [18] revealed that the N and C termini of TP I are folded toward the turn region in the presence of DPC micelles. In contrast, Mizuguchi *et al*. [41] proposed that TP I adopts a straight β-hairpin structure in the presence of DPC micelles (PDB ID 1WO1). Doherty *et al*. [42] reported that no bending is observed in the β-strands of TP I in the lipid bilayer, and concluded that TP I is parallel to the membrane plane and immersed in the interfacial region of the membrane.

In this study, we determined the structure of TP I in its bound state with LPS by the use of Tr-NOESY (Fig. 2b, 4b). Structural analysis revealed that TP I extends its β-sheet structure and stabilizes this structure by binding to LPS. These structural properties were consistent with the results of CD measurements (Fig. 1) that suggested a slight change in the secondary structures of TP I between its free state and LPS-binding state. Intrinsic tryptophan fluorescence studies and fluorescence quenching studies suggested that Trp2 was incorporated into the hydrophobic environment of LPS (Fig. 5). 1D ^{1}H NMR and 1D ^{31}P NMR revealed that the Trp2, Cys3, and Arg17 residues of TP I are involved in binding to LPS, while the phosphate groups of LPS are involved in binding to TP I (Fig. 6, 7). The

complex structure obtained by docking calculation between TP I and LPS showed that TP I lies across the two GlcNs of LPS (Fig. 8). In the complex, cationic residues such as Lys1, Arg15, and Arg17 of TP I interact with the phosphate groups or saccharides of LPS, whereas the aromatic residues Trp2 and Phe4 interact with the acyl chains of LPS. These interaction sites of TP I and LPS shown in complex structure were consistent with the results of intrinsic tryptophan fluorescence and 1D ^{1}H and ^{31}P NMR studies. By binding to LPS, TP I seems to twist its antiparallel β-sheet structure. This conformational change may occur due to the Lys1 and Arg17 residues simultaneously recognizing the same phosphate group of LPS. In other words, a twisting β-sheet structure may be important for TP I to recognize LPS. In fact, few complex structures of TP I and LPS were acquired by docking calculations using the TP I structure in aqueous solution (data not shown).

In recent years, the structure of a TP I mutant in which all four Cys residues were deleted, named CDT, was clarified in its LPS-bound state [19]. Although CDT adopts a random coil conformation in aqueous solution, it adopts a β-hairpin-like structure in the presence of LPS. The Y6-I9 of CDT makes a type II' β-turn and W2-V5 and Y10-R13 are respectively extended. Some side chains of the Arg residues of CDT interact with phosphate groups of lipid A and a hydrophobic surface composed of W2, F3, Y6, I9 and Y10 is inserted along the acyl chains of lipid A.

Comparing the TP I-LPS complex with the CDT-LPS complex, we note several similarities. First, the guanidyl groups of Arg residues located in the C terminus were important for both peptides to interact with the phosphate groups of LPS. Secondly, aromatic residues such as W2 and F4 (F3 in CDT) were inserted into the hydrophobic acyl chains of LPS. However, there were also some differences between the TP I-LPS complex and CDT-LPS complex. In the case of TP I, the side chain of K1 was in close proximity to the phosphate group, but K1 of CDT was not involved in the interaction with the phosphate group. The side chain of R9 of TP I was not close to the phosphate group of LPS, but the side chain of R7 of CDT corresponding to R9 of TPI was in close proximity to the phosphate group of LPS. Further, the backbone and side chains of I9 (I11 in TP I) of CDT were in close proximity to LPS, while I11 of TP I seemed unlikely to be involved in binding to LPS. In addition, the peptide locations in LPS were drastically different. CDT was located at the base of the acyl chains of lipid A, while TP I lay on two glucosamine residues. These differences may suggest that TP I and CDT interact with LPS in distinct ways.

In conclusion, we revealed that binding to LPS slightly extends the two β-strands of TP I and stabilizes the whole structure of TP I. Fluorescence studies indicated that a tryptophan residue is incorporated into the hydrophobic environment of LPS. 1D ^{1}H NMR study suggested that residues located in the N and C termini of TP I were involved in the binding to LPS. 1D ^{31}P NMR measurements suggested that phosphate groups of LPS were in close proximity to TP I. Finally, we proposed the model structure of the complex of TP I with LPS by using a docking program. The calculated model structure suggested that the cationic residues of TP I

interact with the phosphate groups and saccharides of LPS, whereas the hydrophobic residues interact with the acyl chains of LPS. The complex structure of TP I and LPS that we revealed in this report provides detailed structural knowledge about the binding of TP I to LPS. We hope that these findings will be fundamental to elucidating the LPS recognition system of AMPs.

Acknowledgments

This work was supported by JSPS KAKENHI Grant Number 25-2798 and was partially supported by the Programme for Promotion of Basic and Applied Researches for Innovations in Bio-oriented Industry.

References

[1] H. Nikaido, Prevention of drug access to bacterial targets: permeability barriers and active efflux, Science 264 (1994) 382-388.

[2] L. Zhang, M.G. Scott, H. Yan, L.D. Mayer, R.E. Hancock, Interaction of polyphemusin I and structural analogs with bacterial membranes, lipopolysaccharide, and lipid monolayers, Biochemistry 39 (2000) 14504-14514.

[3] J. Cohen, The immunopathogenesis of sepsis, Nature 420 (2002) 885-891.

[4] A. Bhunia, A. Ramamoorthy, S. Bhattacharjya, Helical hairpin structure of a potent antimicrobial peptide MSI-594 in lipopolysaccharide micelles by NMR spectroscopy, Chemistry 15 (2009) 2036-2040.

[5] J. Mares, S. Kumaran, M. Gobbo, O. Zerbe, Interactions of lipopolysaccharide and polymyxin studied by NMR spectroscopy, J. Biol. Chem. 284 (2009) 11498-11506.

[6] D. Sipos, M. Andersson, A. Ehrenberg, The structure of the mammalian antibacterial peptide cecropin P1 in solution, determined by proton-NMR, Eur. J. Biochem. 209 (1992) 163-169.

[7] N. Mandard, P. Sodano, H. Labbe, J.M. Bonmatin, P. Bulet, C. Hetru, M. Ptak, F. Vovelle, Solution structure of thanatin, a potent bactericidal and fungicidal insect peptide, determined from proton two-dimensional nuclear magnetic resonance data, Eur. J. Biochem. 256 (1998) 404-410.

[8] N. Mandard, P. Bulet, A. Caille, S. Daffre, F. Vovelle, The solution structure of gomesin, an antimicrobial cysteine-rich peptide from the spider, Eur. J. Biochem. 269 (2002) 1190-1198.

[9] W. Gong, J. Wang, Z. Chen, B. Xia, G. Lu, Solution structure of LCl, a novel antimicrobial peptide from *Bacillus subtilis*, Biochemistry 50 (2011) 3621-3627.

[10] Y. Huang, J. Huang, Y. Chen, Alpha-helical cationic antimicrobial peptides: relationships of structure and function, Protein Cell 1 (2010) 143-152.

[11] M. Zasloff, Antimicrobial peptides of multicellular organisms, Nature 415 (2002) 389-395.

[12] Q.P. Lin, L.F. Zhou, N.N. Li, Y.Q. Chen, B.C. Li, Y.F. Cai, S.Q. Zhang, Lipopolysaccharide neutralization by the antibacterial peptide CM4, Eur. J. Pharmacol 596 (2008) 160-165.

[13] A. Bhunia, H. Mohanram, S. Bhattacharjya, Lipopolysaccharide bound structures of the active fragments of fowlicidin-1, a cathelicidin family of antimicrobial and antiendotoxic peptide from chicken, determined by transferred nuclear Overhauser effect spectroscopy, Biopolymers 92 (2009) 9-22.

[14] A. Bhunia, P.N. Domadia, J. Torres, K.J. Hallock, A. Ramamoorthy, S. Bhattacharjya, NMR structure of pardaxin, a pore-forming antimicrobial peptide, in lipopolysaccharide micelles: mechanism of outer membrane permeabilization, J. Biol.

Chem. 285 (2010) 3883-3895.

[15] T. Nakamura, H. Furunaka, T. Miyata, F. Tokunaga, T. Muta, S. Iwanaga, M. Niwa, T. Takao, Y. Shimonishi, Tachyplesin, a class of antimicrobial peptide from the hemocytes of the horseshoe crab (*Tachypleus tridentatus*). Isolation and chemical structure, J. Biol. Chem. 263 (1988) 16709-16713.

[16] Y. Hirakura, S. Kobayashi, K. Matsuzaki, Specific interactions of the antimicrobial peptide cyclic beta-sheet tachyplesin I with lipopolysaccharides, Biochim. Biophys. Acta 1562 (2002) 32-36.

[17] K. Kawano, T. Yoneya, T. Miyata, K. Yoshikawa, F. Tokunaga, Y. Terada, S. Iwanaga, Antimicrobial peptide, tachyplesin I, isolated from hemocytes of the horseshoe crab (*Tachypleus tridentatus*). NMR determination of the beta-sheet structure, J. Biol. Chem. 265 (1990) 15365-15367.

[18] A. Laederach, A.H. Andreotti, D.B. Fulton, Solution and micelle-bound structures of tachyplesin I and its active aromatic linear derivatives, Biochemistry 41 (2002) 12359-12368.

[19] R. Saravanan, H. Mohanram, M. Joshi, P.N. Domadia, J. Torres, C. Ruedl, S. Bhattacharjya, Structure, activity and interactions of the cysteine deleted analog of tachyplesin-1 with lipopolysaccharide micelle: Mechanistic insights into outer-membrane permeabilization and endotoxin neutralization, Biochim. Biophys. Acta 1818 (2012) 1613-1624.

[20] J.P. Powers, A. Rozek, R.E. Hancock, Structure-activity relationships for the beta-hairpin cationic antimicrobial peptide polyphemusin I, Biochim. Biophys. Acta. 1698 (2004) 239-250.

[21] F. Delaglio, S. Grzesiek, G.W. Vuister, G. Zhu, J. Pfeifer, A. Bax, NMRPipe: a multidimensional spectral processing system based on UNIX pipes, J. Biomol. NMR 6 (1995) 277-293.

[22] T.D. Goddard, D.G. Kneller, SPARKY 3, University of California, San Francisco

[23] L. Braunschweiler, R.R. Ernst, Coherence transfer by isotropic mixing: Application to proton correlation spectroscopy, J. Magn. Reson. 53 (1983) 521-528.

[24] C.B. Post, Exchange-transferred NOE spectroscopy and bound ligand structure determination, Curr. Opin. Struct. Biol. 13 (2003) 581-588.

[25] C.D. Schwieters, J.J. Kuszewski, N. Tjandra, G.M. Clore, The Xplor-NIH NMR molecular structure determination package, J. Magn. Reson. 160 (2003) 65-73.

[26] C.D. Schwieters, J.J. Kuszewski, G.M. Clore, Using Xplor-NIH for NMR molecular structure determination, Prog. Nucl. Magn. Reson. Spectrosc. 48 (2006) 47-62.

[27] R.A. Laskowski, J.A. Rullmannn, M.W. MacArthur, R. Kaptein, J.M. Thornton, AQUA and PROCHECK-NMR: programs for checking the quality of protein structures solved by NMR, J.Biomol. NMR 8 (1996) 477-486.

[28] The PyMOL molecular graphics system, Version 1.6.0.0 Schrödinger, LLC.

[29] G.M. Morris, R. Huey, W. Lindstrom, M.F. Sanner, R.K. Belew, D.S. Goodsell, A.J. Olson, AutoDock4 and AutoDockTools4: Automated docking with selective receptor flexibility, J. Comput. Chem. 30 (2009) 2785-2791.

[30] A.D. Ferguson, W. Welte, E. Hofmann, B. Lindner, O. Holst, J.W. Coulton, K. Diederichs, A conserved structural motif for lipopolysaccharide recognition by procaryotic and eucaryotic proteins, Structure 8 (2000) 585-592.

[31] L. Yu, M. Tan, B. Ho, J.L. Ding, T. Wohland, Determination of critical micelle concentrations and aggregation numbers by fluorescence correlation spectroscopy: aggregation of a lipopolysaccharide, Anal. Chem. Acta 556 (2006) 216-225.

[32] S.M. Strain, S.W. Fesik, I.M. Armitage, Structure and metal-binding properties of lipopolysaccharides from heptoseless mutants of *Escherichia coli* studied by ^{13}C and ^{31}P nuclear magnetic resonance, J. Biol. Chem. 258 (1983) 13466-13477.

[33] S. Müller-Loennies, O. Holst, B. Lindner, H. Brade, Isolation and structural analysis of phosphorylated oligosaccharides obtained from *Escherichia coli* J-5 lipopolysaccharide, Eur. J. Biochem. 260 (1999) 235-249.

[34] D. Marion, M. Zasloff, A. Bax, A two-dimensional NMR study of the antimicrobial peptide magainin 2, FEBS Lett. 227 (1988) 21-26.

[35] A. Aumelas, M. Mangoni, C. Roumestand, L. Chiche, E. Despaux, G. Grassy, B. Calas, A. Chavanieu, Synthesis and solution structure of the antimicrobial peptide protegrin-1, Eur. J. Biochem. 237 (1996) 575-583.

[36] K. Matsuzaki, Why and how are peptide-lipid interactions utilized for self-defense? Magainins and tachyplesins as archetypes, Biochim. Biophys. Acta 1462 (1999) 1-10.

[37] B.F. Tack, M.V. Sawai, W.R. Kearney, A.D. Robertson, M.A. Sherman, W. Wang, T. Hong, L.M. Boo, H. Wu, A.J. Waring, R.I. Lehrer, SMAP-29 has two LPS-binding sites and a central hinge, Eur. J. Biochem. 269 (2002) 1181-1189.

[38] F. Porcelli, R. Verardi, L. Shi, K.A. Henzler-Wildman, A. Ramamoorthy, G. Veglia, NMR structure of the cathelicidin-derived human antimicrobial peptide LL-37 in dodecylphosphocholine micelles, Biochemistry 47 (2008) 5565-5572.

[39] T.J. Park, J.S. Kim, H.C. Ahn, Y. Kim, Solution and solid-state NMR structural studies of antimicrobial peptides LPcin-I and LPcin-II, Biophys. J. 101 (2011) 1193-1201.

[40] A.G. Rao, Conformation and antimicrobial activity of linear derivatives of tachyplesin lacking disulfide bonds, Arch. Biochem. Biophys. 361 (1999) 127-134.

[41] M. Mizuguchi, S. Kamata, S. Kawabata, K. Kawano, Structure of horseshoe crab antimicrobial peptide, tachyplesin I in dodecylphosphocholine micelles, Pept. Sci. 2002 (2003) 281-282.

[42] T. Doherty, A.J. Waring, M. Hong, Membrane-bound conformation and topology of the antimicrobial peptide tachyplesin I by solid-state NMR, Biochemistry 45 (2006) 13323-13330.

Table 1. Summary of the structural statistics for the 20 lowest energy structures of TP I in its free and LPS-bound state.

	free	+LPS
Distance restraints		
Intra-residue	65	101
Sequential	34	69
Medium-range	2	13
Long-range	9	33
Total	110	216
Angular restraints	15	13
Deviation from mean structure (only for the well-defined region C3-C16)		
Backbone (Å)	0.771	0.632
Ramachandran plot analysis		
% Residues in the most favorable regions	65.7	78.9
% Residues in additionally allowed regions	29.3	20.0
% Residues in generously allowed regions	5.0	1.1
% Residues in disallowed regions	0.0	0.0

Figure Legends

Fig. 1. CD spectra of TP I in the absence (dotted lines) and presence of LPS (solid lines). The concentrations of TP I and LPS were 30 μM and 72 μM in 10 mM sodium phosphate buffer (pH7.4), respectively. Measurements were carried out at 25 ºC.

Fig. 2. (a) The line-broadening by the addition of LPS to TP I solution. The TP I concentration was 750 μM and the LPS concentration was 0 (black), 20 (blue), 35 (green), or 50 μM (red) in 10% D_2O at pH 3.8. These spectra were measured at 35 ºC. (b) Superimposition of the NOESY spectrum of TP I in water and the Tr-NOESY spectrum of TP I containing LPS. Red-colored peaks were observed in the measurement of Tr-NOESY and blue-colored peaks were obtained by the measurement of NOESY. Assigned peaks were observed only in the presence of LPS.

Fig. 3. Histogram showing the number of NOEs of TP I as a function of residues with or without LPS.

Fig. 4. Superimposition of the 20 lowest-energy structures of TP I in water (a) and in the presence of LPS (b). β-strands are shown in green and disulfide bonds are shown in orange.

Fig. 5. (a) Plot showing changes in maximal emission wavelength of the intrinsic tryptophan fluorescence of TP I, as a function of increasing concentrations of LPS. TP I was dissolved in 10 mM sodium phosphate buffer (pH7.4) at a final concentration of 5 μM. (b) Fluorescence quenching of TP I by acrylamide in 10 mM sodium phosphate buffer at pH 7.4 with or without LPS. The concentrations of TP I and LPS were 5 μM and 12 μM, respectively.

Fig. 6. Low-field resonances of 1D ^{1}H NMR spectra of TP I with LPS (red) or without LPS (blue). The TP I and LPS concentrations were respectively 750 μM and 50 μM in 10% D_2O at pH 3.8. These spectra were measured at 35 ºC. The black spectrum represents the difference between the two spectra. Arrows indicate chemical shift changes of TP I by the addition of LPS.

Fig. 7. 1D ^{31}P NMR spectra of LPS with various concentrations of TP I measured at 35 ºC. LPS was dissolved in 10% D_2O, pH 3.8, at a final concentration of 400 μM. The spectra displayed in black, purple, blue and green indicate LPS:TP I molar ratios of 1:0, 1:0.5, 1:1, and 1:1.5, respectively.

Fig. 8. (a) LPS structure used in the docking calculation. GlcN: 3-deoxy-D-glucosamine. (b) The complex structure of TP I and LPS. TP I is shown as a cartoon and (c) sticks. The

docking model was calculated by using the structure of TP I in its LPS-bound state and the crystal structure of LPS (PDB ID 1QFG). Key cationic residues of TP I (K1, R14, R15 and R17) for binding to LPS are shown in blue, and aromatic residues (W2 and F4) interacting with the acyl chains of LPS are shown in green.

Figure 1.

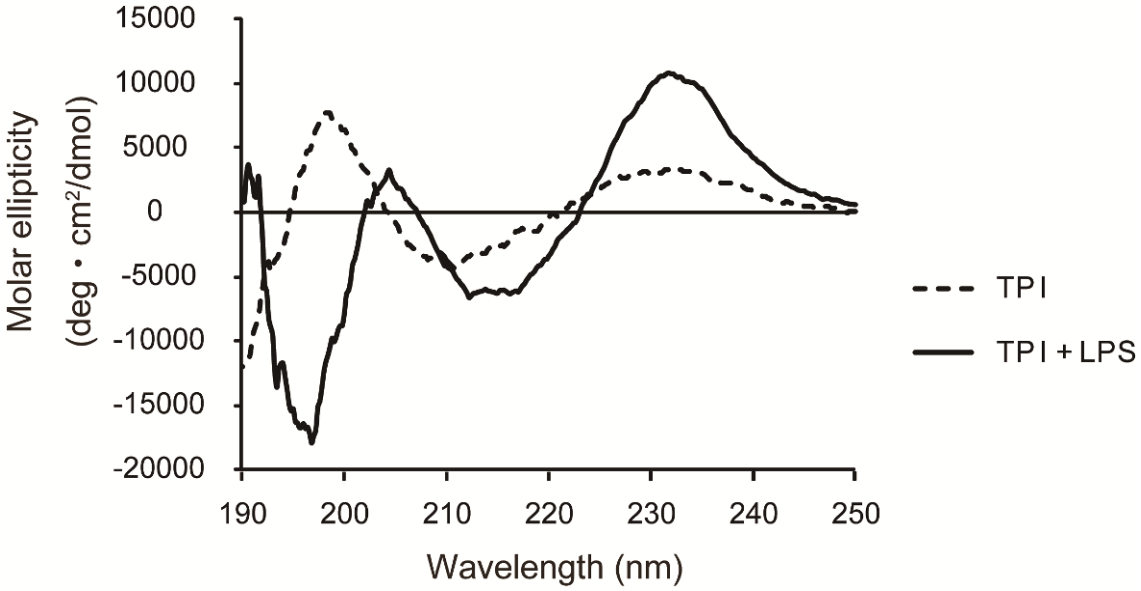
15000
10000
5000
0
-5000
-10000
-15000
-20000
Molar ellipticity
(deg • cm²/dmol)
190
200
210
220
230
240
250
Wavelength (nm)
TPI
TPI + LPS

Figure 2.

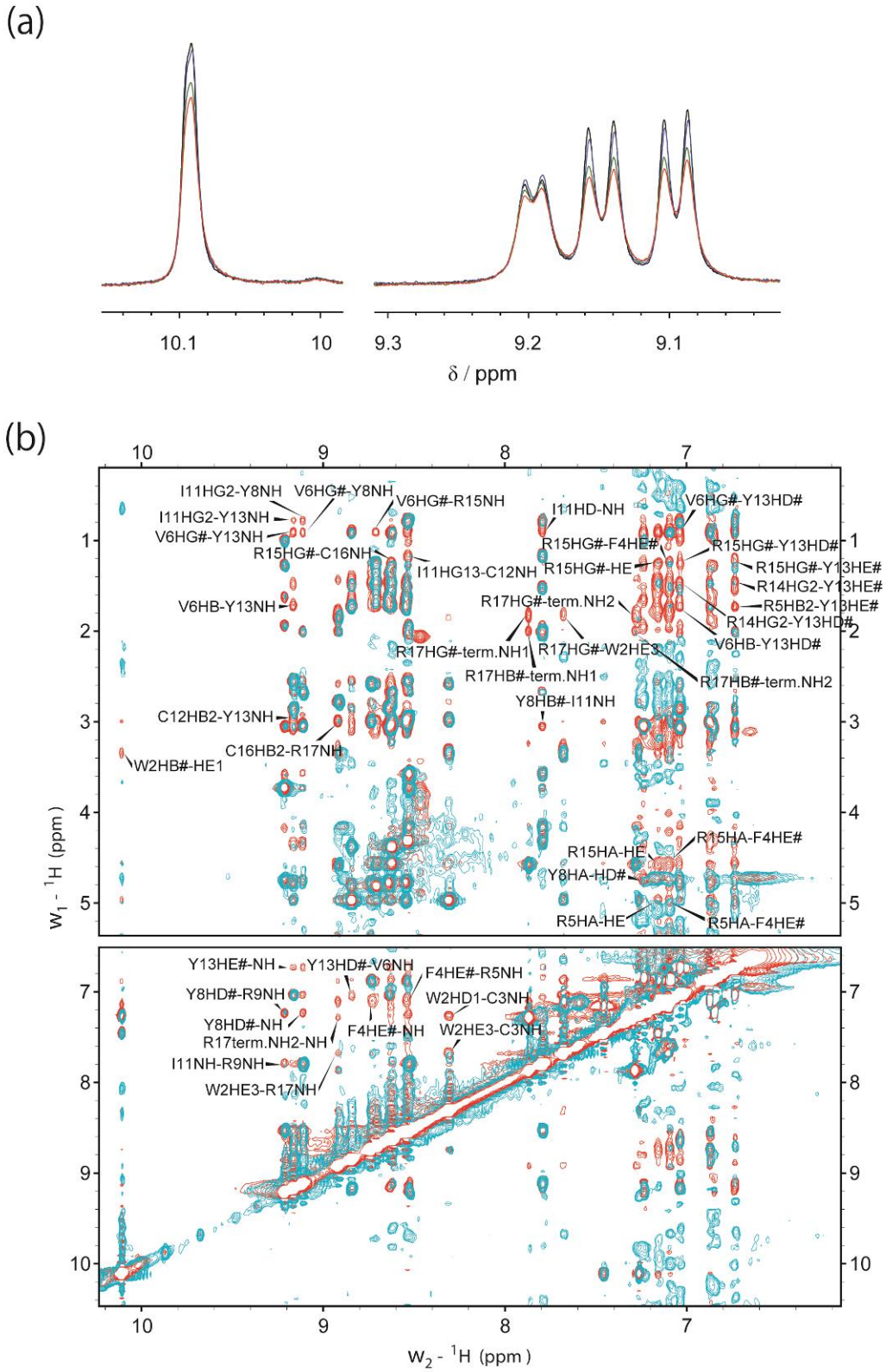
(a)
10.1
10
9.3
9.2
9.1
δ / ppm
(b)
I11HG2-Y8NH
V6HG#-Y8NH
V6HG#-R15NH
I11HG2-Y13NH
V6HG#-Y13NH
R15HG#-C16NH
I11HG13-C12NH
V6HB-Y13NH
R17HG#-term.NH1
C12HB2-Y13NH
C16HB2-R17NH
W2HB#-HE1
I11HD-NH
R15HG#-F4HE#
R15HG#-HE
R17HG#-term.NH2
R17HG#-W2HE3
R17HB#-term.NH1
Y8HB#-I11NH
V6HG#-Y13HD#
R15HG#-Y13HD#
R15HG#-Y13HE#
R14HG2-Y13HE#
R5HB2-Y13HE#
R14HG2-Y13HD#
V6HB-Y13HD#
R17HB#-term.NH2
R15HA-HE
Y8HA-HD#
R5HA-HE
R15HA-F4HE#
R5HA-F4HE#
Y13HE#-NH
Y13HD#-V6NH
Y8HD#-R9NH
Y8HD#-NH
R17term.NH2-NH
I11NH-R9NH
W2HE3-R17NH
F4HE#-NH
F4HE#-R5NH
W2HD1-C3NH
W2HE3-C3NH
W1 - 1H (ppm)
W2 - 1H (ppm)

Figure 3.

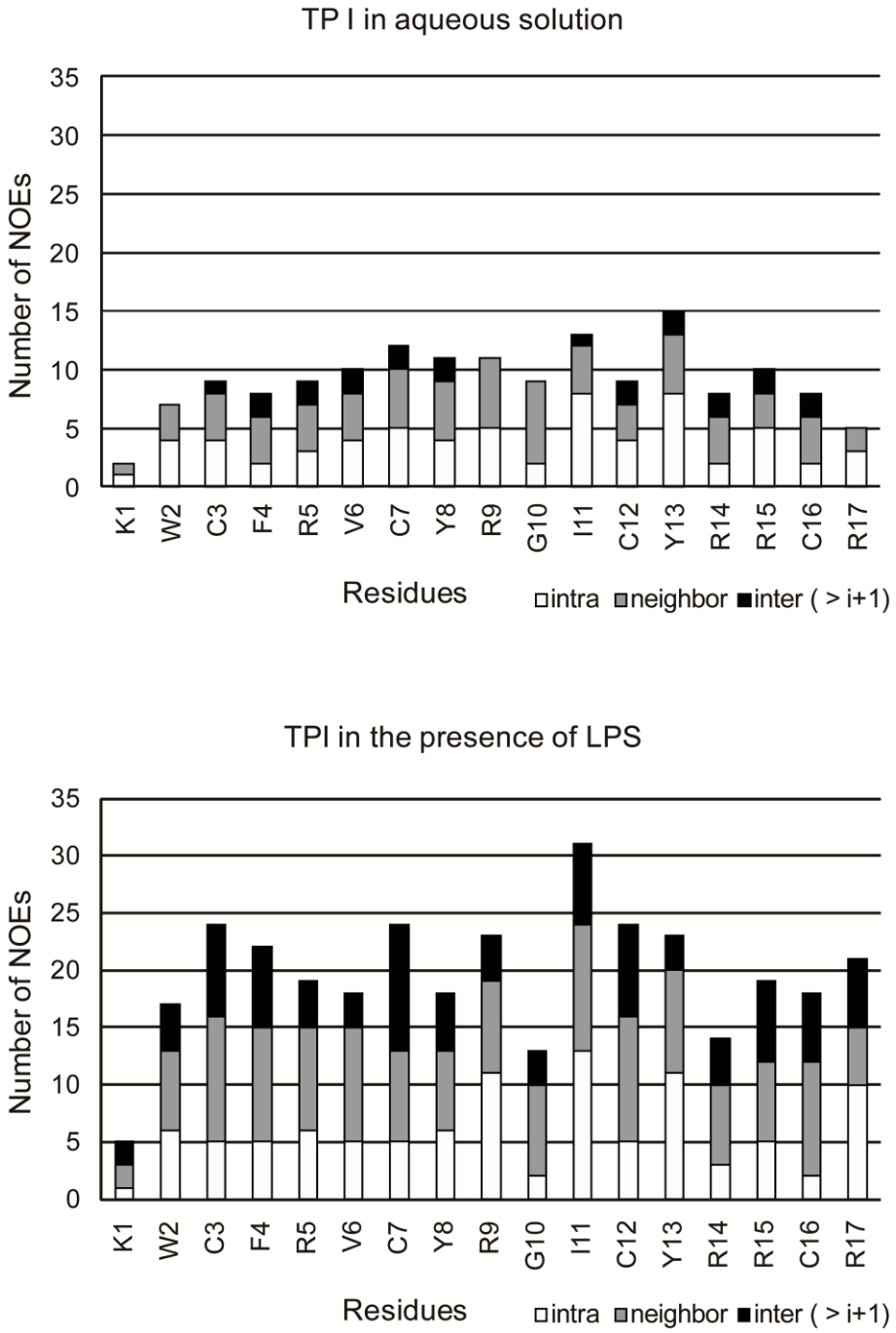
TP I in aqueous solution
Number of NOEs
0
5
10
15
20
25
30
35
K1
W2
C3
F4
R5
V6
C7
Y8
R9
G10
I11
C12
Y13
R14
R15
C16
R17
Residues
intra
neighbor
inter (> i+1)
TPI in the presence of LPS
Number of NOEs
0
5
10
15
20
25
30
35
K1
W2
C3
F4
R5
V6
C7
Y8
R9
G10
I11
C12
Y13
R14
R15
C16
R17
Residues
intra
neighbor
inter (> i+1)

Figure 4.

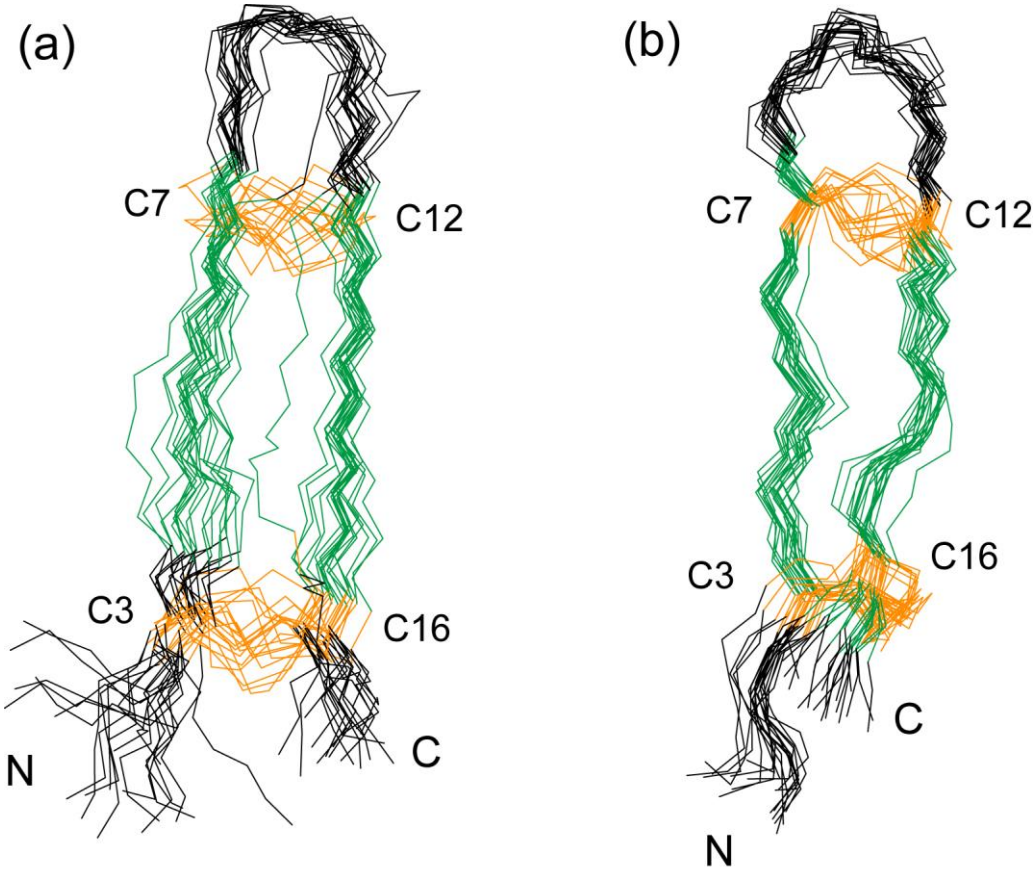

Figure 5.

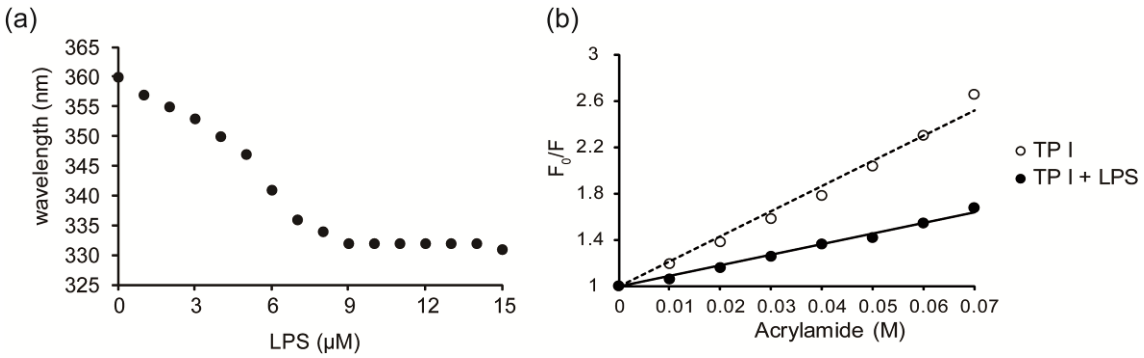
(a)
wavelength (nm)
365
360
355
350
345
340
335
330
325
0
3
6
9
12
15
LPS (μM)
(b)
F_0/F
3
2.6
2.2
1.8
1.4
1
0
0.01
0.02
0.03
0.04
0.05
0.06
0.07
Acrylamide (M)
TP I
TP I + LPS

Figure 6.

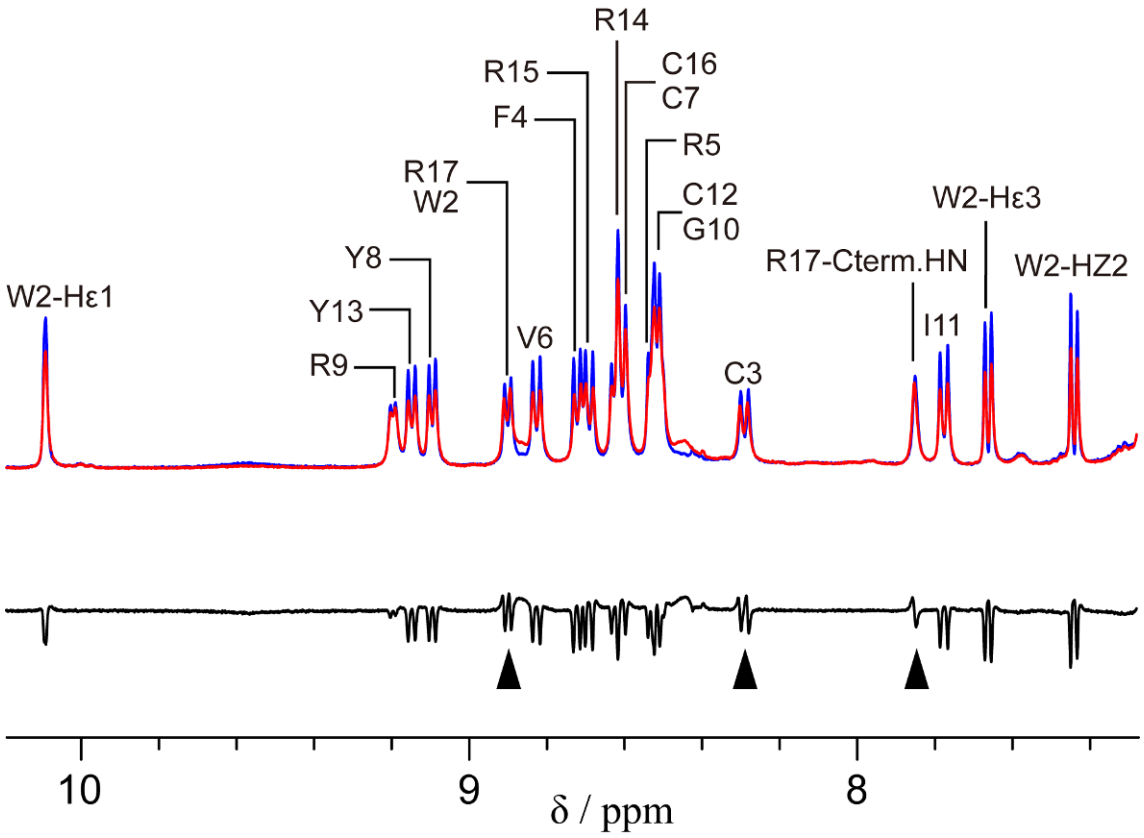
R14
R15
C16
C7
F4
R5
R17
W2
C12
G10
W2-Hε3
Y8
R17-Cterm.HN
W2-HZ2
W2-Hε1
Y13
V6
I11
R9
C3
10
9
8
δ / ppm

Figure 7.

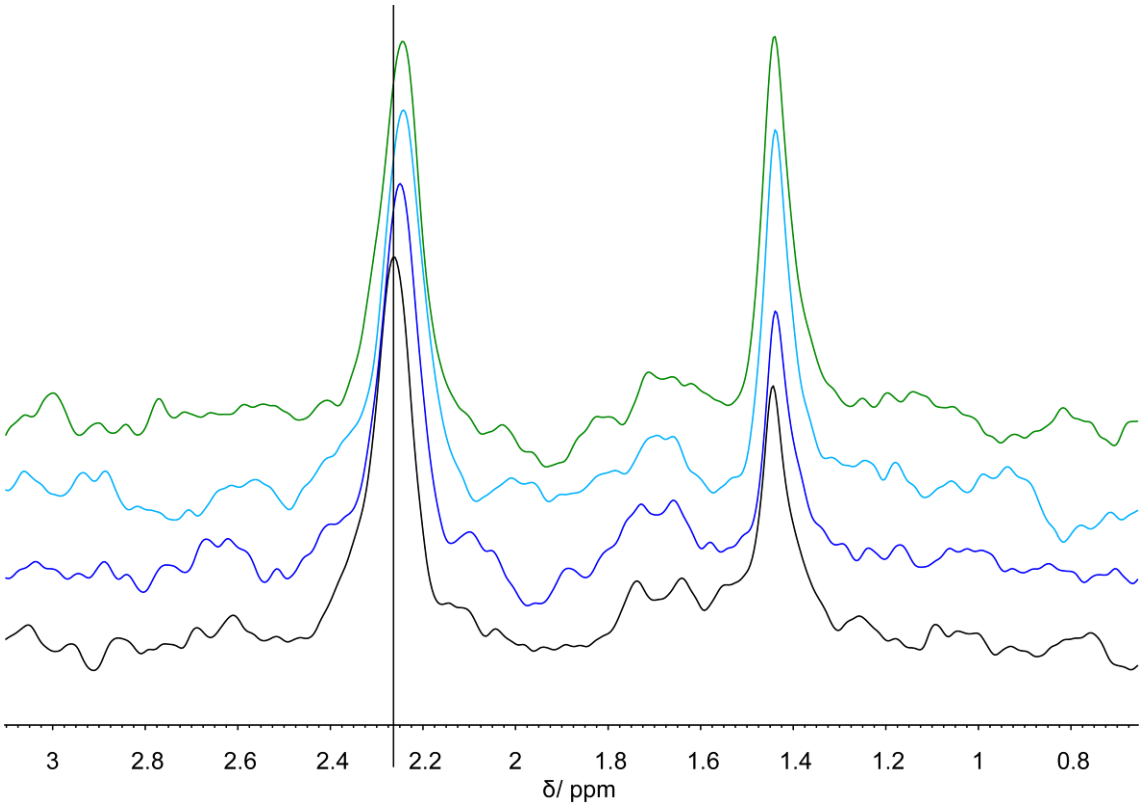

Figure 8.

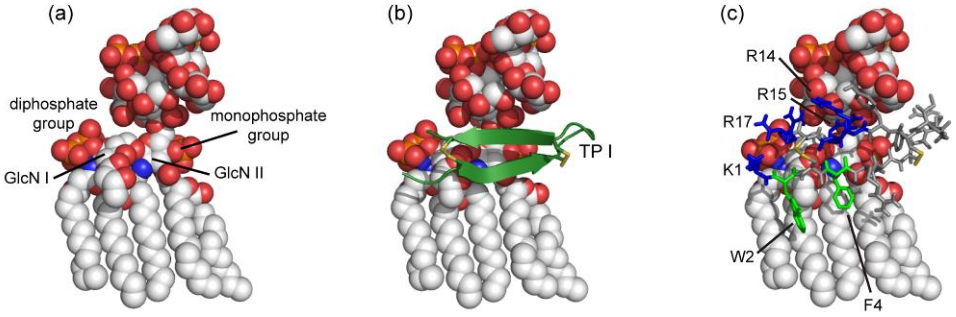
(a)
diphosphate group
monophosphate group
GlcN I
GlcN II
(b)
TP I
(c)
R14
R15
R17
K1
W2
F4